COMPUTATIONAL INVESTIGATION OF THE EFFECT OF CLUSTER IMPACT ENERGY ON THE MICROSTRUCTURE OF FILMS GROWN BY CLUSTER DEPOSITION

AVINASH M. DONGARE, DEREK D. HASS, and LEONID V. ZHIGILEI
Department of Materials Science & Engineering, University of Virginia, Charlottesville, Virginia 22904-4745
E-mail: davinash@virginia.edu

The microstructure of thin film growth during low-energy cluster beam deposition is studied in a series of molecular dynamics simulations. The films are grown by depositing Ni clusters on a Ni (111) substrate at room temperature. The deposition of a single Ni cluster is first studied, followed by a detailed analysis of the effect of the impact velocity of the deposited clusters on the microstructure of the growing film. The observed differences in the microstructure are related to the differences in the impact-induced processes. In the case of the lower incident energy only a partial transient melting of a small contact region between the incoming cluster and the film takes place. Epitaxial growth is seen to occur for the first few layers of the clusters in contact with the substrate, above which the clusters largely retain their crystal structure and orientation. The films grown by deposition of low-energy clusters have a low density (~50% of the density of a perfect crystal) and a porous "foamy" structure with a large number of interconnected voids. The higher-energy impacts lead to the complete melting and recrystallization of the whole cluster and a large region of the film, leading to the epitaxial growth, smaller number of localized voids, and a higher overall density of the growing film.

1. Introduction

Cluster deposition is one of the major methods used in fabrication of nanostructured materials with unique range of optical, magnetic, mechanical and catalytic properties [1]. One of the commonly used nanofabrication techniques is the low-energy cluster beam deposition (LECBD) method, in which the materials are grown by a controlled deposition of clusters with a narrow size distribution, typically in the range from 1 to 10 nm. Different techniques used for generation of clusters beams, such as multiple-expansion cluster source (MECS) [2], gas segregation technique [3], electron beam direct vapor deposition (EB-DVD) [4], and laser vaporization cluster source [5], offer different degrees of control over the cluster size and energy distributions. From the point of view of fabrication of nanostructured materials it is often desirable to retain the characteristic length-scale and high surface/volume ratio of the deposited clusters in the cluster-assembled material and, at the same time, to form a continuous and mechanically stable material. To achieve the desired properties of the growing films, the parameters of the deposition process should be chosen based on the understanding of the fundamental atomic-level processes leading to the formation of the final microstructure.

The Molecular Dynamics (MD) simulation technique has been demonstrated to be capable of providing insights into the mechanisms of cluster-substrate interaction [6,7,8,9,10] as well as the relation between the parameters of the deposited clusters and the microstructure of the deposited films [10,11,12,13,14]. It has been observed that the final state of a deposited cluster depends on the size and the incident energy of the cluster, with partial "contact epitaxy" characteristic for low-energy "soft landing" of large clusters and complete epitaxy characteristic for smaller and/or more energetic clusters [7,8,9,10]. Simulations of the film growth by cluster deposition revealed a strong dependence of the morphology of the growing film on deposition parameters. In particular, Haberland, Insepov and Moseler [11] investigated the structure of thin films grown by deposition of 1043-atomic Mo clusters. They observed a transition from a porous film with multiple voids to a dense epitaxial film with a nearly bulk density as the incident energy increased from 0.1 eV/atom to 1 eV/atom and to 10 eV/atom. More recently Hou et al. performed MD simulations of film growth by deposition of Ni_3Au clusters on Ni and Al substrates with an impact energy of 0.25 eV/atom [13] and observed only a minor epitaxy with the substrates. Kang et al. studied film growth by deposition of small 177-atomic Al and Cu clusters and observed formation of epitaxial films at sufficiently high impact energies [14].

While the first MD simulations of cluster deposition clearly indicate that the impact energy of the deposited clusters has a strong effect on the structure and density of the growing film, further progress is needed in understanding of the dependence of the morphology and defect structures in the deposited films on the parameters of the deposited cluster. One question of a particular interest is the possibility to generate dense nanocrystalline films by cluster deposition. In this work we report the results of a series of MD simulations aimed specifically at the transition regime from the cluster assembly into an open low-density structure to a compact film with the density approaching that of the bulk. The impact-induced processes are analyzed and related to the density, morphology and microstructure of the growing films. Computational model used in the present study and parameters of the simulations are described below, in Section 2. The results on the film growth by cluster deposition are presented in Section 3 and summarized in Section 4.

2. Computational Model

We simulate deposition of Ni clusters on Ni (111) surface. The clusters are ~3 nm in diameter (532 atoms), which is a typical size of clusters in LECBD experiments [5]. The initial cluster is created by cutting a sphere of the

desired radius from an fcc bulk crystal. The substrate is represented by eight atomic Ni (111) planes, each consisting of 1152 atoms. Periodic boundary conditions are applied in the directions parallel to the surface. Two bottom atomic layers of the substrate are kept rigid. The atoms in a stochastic region adjacent to the rigid layers experience the forces due to the interaction potential as well as friction and stochastic forces via the Langevin equation method [15]. The stochastic region is used for maintaining the constant temperature of the substrate and for an effective simulation of the dissipation of the energy deposited by cluster impacts due to the fast electronic heat conduction. The thickness of the stochastic region is increasing as the thickness of the film growth during the deposition process. The atoms in the topmost region of the system are experiencing only forces due to the interatomic interaction, described in this work by the Embedded Atom Method (EAM) potential in the form and parameterization suggested by Johnson and co-workers [16].

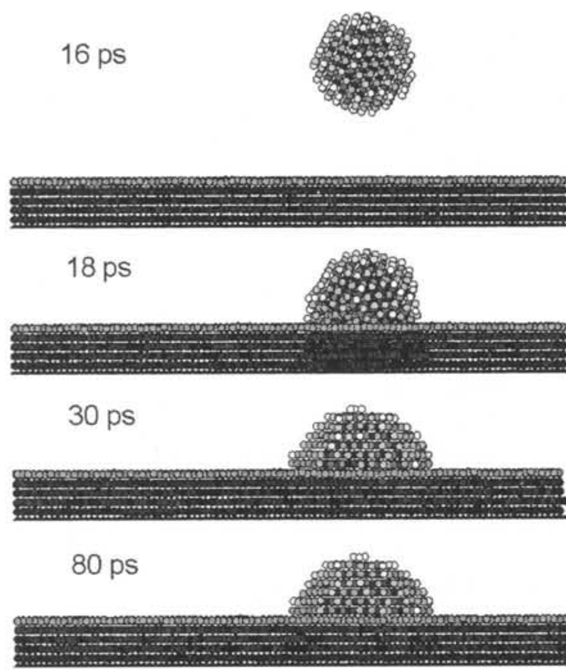

Figure 1. Snapshots from a simulation of the deposition of a single Ni cluster on a Ni (111) substrate at an impact velocity of 1000 m/s. The gray scale corresponds to the potential energy of each atom, from 3.25 eV for white color to 4.43 eV for black color (cohesive energy of the EAM Ni fcc crystal is 4.45 eV).

Prior to the deposition, both cluster and the substrate are equilibrated at 300 K for 10 ps. The positions of the deposited clusters are chosen at random in the x-y plane. The orientation of the cluster with respect to the substrate is also chosen at random. The z coordinate of the cluster is chosen so that the top atoms of the growing film do not interact with the cluster being deposited. The clusters are directed towards the substrate at different impact velocities representing three different cases studied in this work. Simulations are performed for impact velocities of 250 m/s (0.01 eV/atom), 500 m/s (0.076 eV/atom), and 1000 m/s (0.3 eV/atom). The time between the depositions of two consecutive clusters is chosen so that the substrate and the deposited cluster can relax completely and the temperature of the impact region stabilizes at 300 K.

The time between the cluster depositions is decided by investigation of cluster-substrate interaction in deposition of the first cluster, as shown in Figure 1 for a simulation performed for the incident velocity of 1000 m/s. As the cluster impacts the substrate, melting occurs in the cluster and in a part of the substrate as shown in the snapshot for 18 ps. Recrystallization of the substrate and the cluster occurs within the next 10 ps and the deposited cluster material forms an epitaxial island on the substrate, as apparent from the snapshot shown for 30 ps. Similar observations of the epitaxial regrowth of a cluster melted upon impact have been reported for deposition of energetic Au [9,10] and Cu [7] clusters. Only partial epitaxy has been reported for large clusters deposited at low impact energies [8,9]. We find that the tendency to form an epitaxial island also depends on the potential used in the simulation. For the conditions illustrated in Figure 1 we observe only partial epitaxy in a simulation performed with a pair-wise Lennard-Jones potential parameterized for Ni [17].

Comparison of the snapshots shown in Figure 1 for 30 ps and 80 ps indicate that the active processes of atomic rearrangements are finished by the time of 30 ps and the temperature of the impact region has decreased down to the temperature of the substrate, 300 K. The mobility of atoms and clusters on the surface can be neglected at 300 K [10,11] and further relaxation of the deposited atomic configurations should not lead to any significant changes in the morphology and microstructure of the deposited films. Therefore, the time between depositions of clusters in simulations of film growth described in the next section is chosen to be 40 ps.

3. Results and Discussion

Simulation results reported in this paper are obtained for three different impact velocities, 250 m/s (0.01eV/atom), 500 m/s (0.076 eV/atom), and

1000 m/s (0.3 eV/atom). The time between cluster depositions is chosen so that the growing film is completely relaxed after each cluster deposition, as discussed above, in Section 2. The total number of the deposited clusters is chosen so that the thickness of the film would be sufficient to perform analysis of the microstructure and density of the growing material. The visual pictures of the final deposited films and density distributions are shown in Figures 2, 3 and 4 for the three impact velocities.

Figure 2(a) shows the atomic configuration of the film created by the deposition of 55 clusters at a velocity of 250 m/s (0.01 eV/atom). A mere visual inspection of the atomic configuration indicates that the deposited film has an open "foamy" structure with a large number of interconnected voids separated by polycrystalline material with characteristic size comparable to the size of the deposited clusters. Epitaxial ordering of the deposited atoms can be identified only in the first few monolayers of the deposited material adjacent to the substrate (~3-5 nm). While the deposited clusters do not melt or disintegrate upon impact, they tend to reorient and adjust to the existing facets, forming crystallites that are larger than the size of an individual cluster. Large number of crystal defects, such as stacking faults, twinning planes, and grain boundaries, can be identified in the atomic configuration. The voids that are created by random deposition of clusters do not collapse with the deposition of the following incoming clusters. The overall density of the film grown at this low-impact velocity is ~50% of the density of the perfect fcc crystal, as can be seen from Figure 2(b).

Figure 3(a) shows the morphology of a film created by the deposition of 55 clusters at a higher velocity of 500 m/s (0.076 eV/atom). It can be seen that as the impact energy of the deposited clusters increases, the porosity of the film decreases. While relatively large voids are observed in the atomic configuration, they are less connected with each other and are separated by solid regions that are significantly thicker as compared to the size of the deposited clusters. Epitaxial growth is seen to occur for a greater thickness (~7-8 nm) as compared to the lower-energy simulation illustrated in Figure 2(a). The formation of a more compact film can be related to the higher energy of the deposited clusters, sufficient to induce melting of a significant part of the cluster and cause substantial atomic rearrangements in the vicinity of the impact region. The size of the voids created by random cluster deposition is decreasing due to the atomic rearrangements induced by the subsequent cluster depositions. Similarly to the films deposited at a lower impact energy of 0.01 eV/atom, a high density of defects can by identified in the atomic configuration shown in Figure 3(a). The density distribution of the film is shown in Figure 3(b). After formation of a thin ~2 nm high-density layer adjacent to the substrate, the density of the growing film stabilizes at ~60% of the density of the bulk crystal.

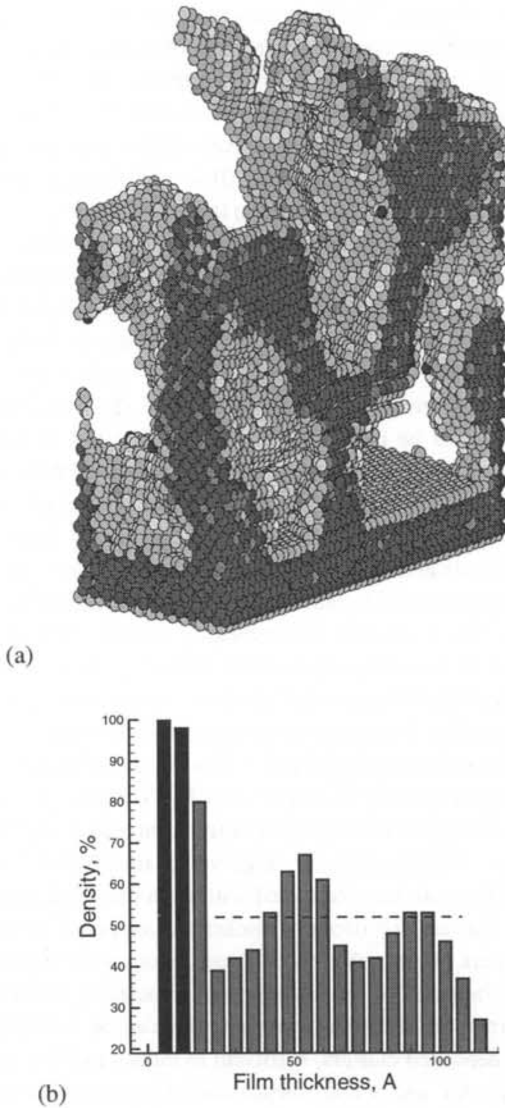

Figure 2. (a) Atomic structure of the film grown by deposition of 55 Ni clusters on the Ni (111) substrate with an impact velocity of 250 m/s. The gray scale corresponds to the potential energy of each atom, from 3.25 eV for white color to 4.43 eV for black color (cohesive energy of the EAM Ni fcc crystal is 4.45 eV). (b) The density distribution of the deposited film. The first two columns (black) correspond to the original substrate. Dashed line shows the average density of the deposited film.

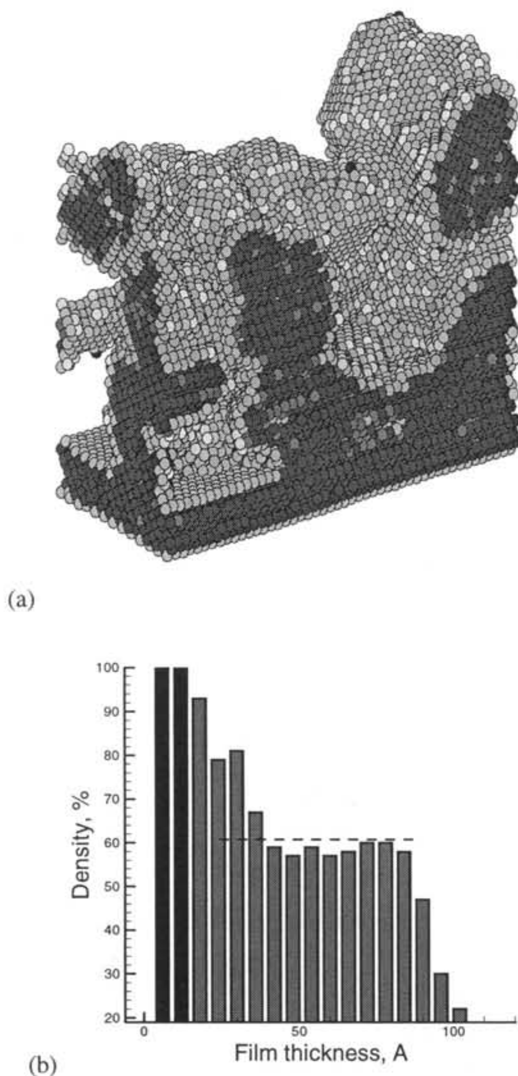

Figure 3. (a) Atomic structure of the film grown by deposition of 55 Ni clusters on the Ni (111) substrate with an impact velocity of 500 m/s. The gray scale corresponds to the potential energy of each atom, from 3.25 eV for white color to 4.43 eV for black color (cohesive energy of the EAM Ni fcc crystal is 4.45 eV). (b) The density distribution of the deposited film. The first two columns (black) correspond to the original substrate. Dashed line shows the average density of the deposited film.

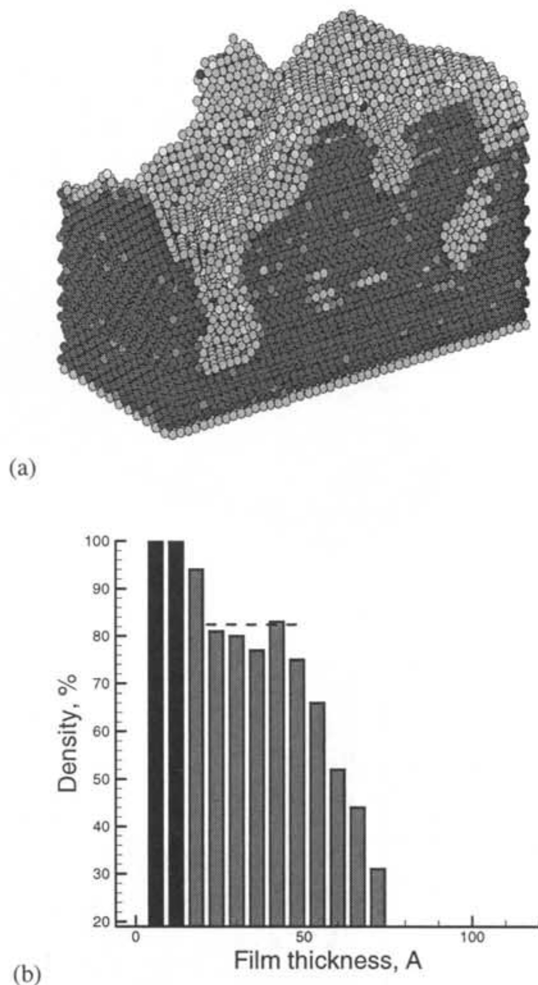

Figure 4. (a) Atomic structure of the film grown by deposition of 45 Ni clusters on the Ni (111) substrate with an impact velocity of 1000 m/s. The gray scale corresponds to the potential energy of each atom, from 3.25 eV for white color to 4.43 eV for black color (cohesive energy of the EAM Ni fcc crystal is 4.45 eV). (b) The density distribution of the deposited film. The first two columns (black) correspond to the original substrate. Dashed line shows the average density of the deposited film.

Figure 4(a) shows the morphology of the film after the deposition of 45 clusters at a velocity of 1000 m/s (0.3 eV/atom). At this deposition velocity almost complete epitaxy is observed, which is consistent with earlier observations for films produced by high-energy cluster deposition [11,14]. The higher-energy impacts lead to the complete melting of the whole cluster and a large region of the film, leading to the epitaxial regrowth of the surrounding crystalline material. As a result, the epitaxial ordering can be observed in the whole deposited film and only several relatively small isolated voids are present in the atomic configuration. The density of the growing film is ~85% of the density of the perfect crystal as can be seen from Figure 4(b). While significant number of low-energy defects (stacking faults and twin boundaries) can be identified in the atomic configuration, the original orientation of (111) planes in the substrate is retained throughout the deposited film.

4. Conclusions

The effect of the impact velocity of the deposited clusters on the morphology and microstructure of the growing films is studied in a series of MD simulations. We find that low-energy deposition results in the formation of open structures with a large number of interconnected voids and large surface-to-volume ratio. The crystalline regions have crystallographic orientation independent from the one of the original substrate and have characteristic sizes comparable to (and somewhat larger then) the size of the deposited clusters. The increase of the cluster impact energy leads to the formation of more compact/dense films with increasingly large epitaxial region adjacent to the substrate and with smaller voids that become isolated from each other. The density of the deposited films is increasing from ~50% to ~60% and to ~85% as the impact energy of the deposited clusters increases from 0.01 eV/atom to 0.076 eV/atom and to 0.3 eV/atom.

The observed difference in the microstructure of the growing films is a reflection of the difference in the impact-induced processes. In the case of the lower incident energies (250 m/s and 500 m/s) only a partial transient melting of a contact region between the incoming cluster and the film takes place and clusters tend to retain their crystal structure and orientation. The voids that are formed by random cluster deposition do not collapse with the deposition of more clusters at these low energies. On the contrary, the higher-energy impacts (1000 m/s) lead to the complete melting and recrystallization of the whole cluster and a large region of the film, leading to the epitaxial growth, smaller number of voids, and higher overall density of the growing film. Formation of a compact/dense nanocrystalline material appears to be hardly achievable by the direct cluster deposition.

The investigations of cluster deposition performed for a fixed size of the deposited clusters and impact energy can provide first useful insights into the mechanism of thin film growth. In experiments, however, the deposited clusters typically have a range of sizes and impact velocities, e.g. [5,18]. Moreover, the clusters are often co-deposited with monomers. On the modeling side, this calls for application of multiscale computational approaches, where the processes of cluster formation are investigated and the parameters of the deposited clusters (velocity and size distributions, internal temperatures of the clusters) are used as a realistic input in simulations of film growth. Multiscale computational approach for simulation of cluster formation in laser ablation/vaporization and subsequent film deposition has been recently discussed [19,20]. The processes responsible for cluster generation in laser ablation can be investigated in a combined MD – Direct Simulation Monte Carlo (DSMC) simulations [21,22]. The parameters of the ejected ablation plume can be used in MD simulations of film deposition, providing a direct connection between the parameters of the ejected clusters and laser irradiation conditions.

Acknowledgement

Partial financial support of this work was provided by the National Science Foundation through the Materials Research Science and Engineering Center for Nanoscopic Materials Design at the University of Virginia.

References

[1] P. Jensen, Rev. Mod. Phys. **71**, 1695 (1999)

[2] D. M. Schaefer, A. Patil, , R. P. Andres, and R. Reifenberger, Phys. Rev. B **51**, 5322 (1995)

[3] C. G. Granqvist and R. A. Buhrman, J. Appl. Phys. **47**, 2200 (1976)

[4] D. D. Hass and H. N. G. Wadley, in preparation.

[5] L. Bardotti, B. Prével, P. Mélinon, A. Perez, Q. Hou, and M. Hou, Phys. Rev. B **62**, 2835 (2000)

[6] H.-P. Chen and U. Landmann, J. Phys. Chem. 98, 3527 (1994)

[7] H. L. Lei, Q. Hou, and M. Hou, J. Phys.: Condens. Matter **12**, 8387 (2000)

[8] M. Yeadon, M. Ghaly, J. C. Yang, R. S. Averback, J. M. Gibson, Appl. Phys. Lett. **73**, 3208 (1998)

[9] M. Hou, Nucl. Instrum. Methods Phys. Research B **135**, 501 (1998)

[10] Q. Hou, M. Hou, L. Bardotti, B. Prével, P. Mélinon, and A. Perez, Phys. Rev. B **62**, 2825 (2000)

[11] H. Haberland, Z. Insepov, and M. Moseler, Phys. Rev. B **51**, 11061 (1995)

[12] C. L. Kelchner and A. E. DePristo, Nanostruct. Mat. **8**, 253 (1997)

[13] M. Hou, V. S. Kharlamov, E. E. Zhurkin, Phys. Rev. B **66**, 195408 (2002)

[14] J. W. Kang, K. S. Choi, J. C. Kang, E. S. Kang, K. R. Byun, and H. J. Hwang, J. Vac. Sci. Technol. A **19**, 1902 (2001)

[15] M. Berkowitz and J.A. McCammon, Chem. Phys. Lett. **90**, 215 (1982)

[16] X. W. Zhou, H. N. G. Wadley, R. A. Johnson, D. J. Larson, N. Tabat, A. Cerezo, A. K. Petford-Long, G. D. W. Smith, P. H. Clifton, R. L. Martens, and T. F. Kelly, Acta Mater. **49**, 4005 (2001)

[17] T. Halicioğlu and G. M. Pound, Phys. Stat. Sol. **30**, 619 (1975)

[18] L. V. Zhigilei, Appl. Phys. A **76**, 339 (2003)

[19] H. Mizuseki, Y. Jin, Y. Kawazoe, and L. T. Wille, Appl. Phys. A **73**, 731 (2001)

[20] L. V. Zhigilei and A. M. Dongare, Computer Modeling in Engineering & Sciences **3**, 539 (2002)

[21] L. V. Zhigilei, E. Leveugle, B. J. Garrison, Y.G. Yingling, M. I. Zeifman, Chem. Rev. **103**, 321 (2003)

[22] M. I. Zeifman, B. J. Garrison, and L. V. Zhigilei, J. Appl. Phys. **92**, 2181 (2002)